Rec'd 3/26/90

Nitrogen Oxide Abatement by Distributed Fuel Addition

Contract DE-AC22-87PC79850

DOE/PC/79850--10

DE92 005212

Quarterly Report No. 10

for Period

November 1, 1989 through January 31, 1990

Prepared by

J. O. L. Wendt and J. B. Mereb
Department of Chemical Engineering
University of Arizona
Tucson, Arizona 85721

Submitted to

Diane Revay Madden, Project Officer
Environmental Control Technology Division
Pittsburgh Energy Technology Center
Department of Energy

February 1, 1990

ABSTRACT

Mechanisms governing the inter-conversion and destruction of nitrogenous species in the fuel rich reburning zone of a laboratory coal combustor were explored. Emphasis was on a configuration in which the primary flame was of pulverized coal and the reburning fuel was natural gas, although other fuels were also considered. The objective was to extract models to be used in estimating reburning effectiveness in practical combustors.

Reburning mechanisms occur in two regimes; one in which fast reactions between NO and hydrocarbons are usually limited by mixing; the other in which reactions have slowed and in which known gas phase chemistry controls. For the latter regime, a simplified model based on detailed gas phase chemical kinetic mechanisms and known rate coefficients was able to predict temporal profiles of NO, NH_3 and HCN. Reactions with hydrocarbons played important roles in both regimes and the Fenimore N_2 fixation reactions limited reburning effectiveness at low primary NO values.

INTRODUCTION

Reburning[1] is an NO_x abatement technique in which secondary fuel is injected downstream of the fuel lean primary combustion zone of a pulverized coal boiler. The second stage or reburning zone is usually operated at overall fuel rich conditions, allowing a significant fraction of the primary NO to be destroyed to form N_2 and other nitrogenous species. A third zone, in which additional air is introduced, allows an overall fuel lean environment to be attained. This form of NO_x abatement has been applied to full scale units[2,3] and appears to be especially attractive when natural gas is used as the reburning fuel to destroy pollutants created from pulverized coal combustion.

The research reported here is concerned with quantitative delineation of mechanisms that control the destruction and formation of all nitrogenous species in the reburning zone downstream of a pulverized coal flame in a laboratory combustor. The focus is on natural gas reburning with the objective of creating engineering models that are both fundamentally based and yet are sufficiently simple so that they can be used in more complex models of practical combustors. To this end, experiments were conducted in a laboratory downflow pulverized coal combustion configuration that contained the temperature and time attributes of practical combustors, but was still sufficiently well defined to allow the extraction of mechanisms.

In a comprehensive previous study, Chen et al.[4] focussed on parametric studies that allowed the factors determining the ultimate effectiveness of reburning to be delineated. In that work, the primary flue gas resulted from doped gas combustion, and a wide variety of reburning fuels was examined. For nitrogen free reburning fuels, improved mixing in the reburn zone was beneficial to the NO destruction process. Subsequent work by Lanier et al.[5], identified critical mechanisms controlling the destruction of NO during reburning in a package boiler simulator. The destruction of N_2 by hydrocarbon reactions to form HCN was proposed as a mechanism that would limit the effectiveness of reburning, especially at lower primary NO levels. Using a model that did not account for hydrocarbon reactions, Knill and Morgan[6] were able to predict the destruction of NO and HCN for selected experiments in an isothermal drop tube reactor. None of the previous works yielded a mechanism that was able quantitatively to predict profiles of all nitrogenous species (NO, HCN and NH_3) in the reburning zone for all tests. The following specific issues still remain to be resolved: what is the relative contribution of hydrocarbons versus other combustible species in governing NO destruction? What controls the formation and destruction of HCN at both high and low primary NO values and what are the key salient mechanisms describing the formation and destruction of NH_3, HCN and NO in the reburning zone for a pulverized coal primary flame?

Mechanisms governing the destruction of NO in the far fuel rich post flame of a pulverized coal staged combustion system were delineated by Bose and Wendt[7]. They based their analysis on the pioneering fundamental gas phase kinetics studies of others (Glarborg et al.[8], Fenimore[9], Haynes[10,11] among others). This work extends their analysis to a reburning configuration, and expands the analysis to predict both HCN and NH_3 concentrations as well. Bose and Wendt used measured values of NH_3 in their mechanism. Furthermore, reburning of a coal combustion flue gas by natural gas is a very different configuration from that examined in previous work[7], especially as far as temperature regimes, local hydrocarbon concentrations, and possible mechanisms controlling HCN profiles are concerned.

EXPERIMENTAL COMBUSTOR

Space limitations preclude other than a very brief discussion of the 15 cm ID laboratory combustor, which is similar to that described elsewhere[7]. One minor difference, however, is that to prolong service time, the inner layer of vacuum formed alumina cylinders was replaced by a layer of silicon carbide refractory. In essence, the combustor allowed self sustaining combustion of 1-2 kg/h coal with no external heating, in a plane flame configuration that was representative of full scale units in terms of temperature time history. It was designed to fill the gap between fundamental flat flame or drop tube studies and pilot scale tests.

The first stage (pulverized coal) was operated fuel lean and reburning (secondary) fuel (natural gas, CO or H_2) was injected downstream. The design of the injector is important, however, since mixing is a key variable in determining reburning effectiveness. Ours evolved as a result of many tests and was designed to produce temperature and species profiles that were independent of radius at the first port downstream of the injection port. The injector tip itself was supported in a water cooled, stainless steel probe and consisted of 8 holes, each of 0.14 cm in diameter aligned radially with respect to the probe axis. Variable amounts of N_2 were added to the reburn fuel to produce hole exit velocities that were at least 70 times the bulk primary flue gas velocity. This resulted in adequate mixing within 0.18 s, beyond which radial profiles demonstrated that the furnace did exhibit plug flow reactor behavior, at least as far as temperature and concentration profiles were concerned.

Analyses of major (O_2, CO, CO_2 and H_2) and minor (CH_4, C_2H_6, C_2H_2, NO, HCN, and

NH_3) species were obtained using a water cooled, water quenched probe, continuous emission monitors, a gas chromatograph furnished with TC and FID detectors, and ion and gas specific electrodes as described in previous work[7]. Temperature measurements were made using an uncoated Type R thermocouple, corrected for radiation losses. Time resolution of temperature and species profiles was determined by the distance between access ports in the combustor (0.3 - 0.4 s). Therefore, quantitative comparison between fundamentally based models and data is most appropriate for conditions under which species are changing in those time scales.

The coal used for the primary flame was a Utah Bituminous Coal, the composition of which is given by Bose et al.[7].

RESULTS

In all, 14 runs under various conditions, with various reburning fuels , were completed. Reburning fuel was injected 0.5 - 0.6 s downstream from the primary coal flame. The reburning zone profiles shown here have been extracted from all this experimentation, and are typical. Figure 1 shows temperature and nitrogenous species profiles for three cases in which the primary flame was coal and the reburning fuel was natural gas. Time zero is the inlet to the reburning zone where the primary NO (not depicted on the graphs in order to maintain appropriate scales) is noted in each figure. At this point attention should be focussed on the data points only, not on the lines, which pertain to a model discussed later. Clearly, there are two regimes which come under consideration. First, for the regime covered by the profiles on the graph, there are no mixing complications, and species change over fairly long time scales. Second, between the inlet to the reburning zone (NO_p) and the first data point there is a very rapid destruction of NO, and here mixing effects might be important, since time scales are short (within 0.18 s). Note the rise of HCN and NH_3 in the slow kinetic regime.

Figure 2 shows reburning zone profiles for CO and H_2 as the reburning fuels. Here the primary NO is shown on the graph, and the fast regime demonstrates only a little NO destruction, which continues through the slow regime. The HCN and NH_3 values are extremely small (less than 7 ppm for HCN and less than 16 ppm for NH_3) which is to be expected. That these species exist at all is surprising since hydrocarbon values in the reburning zone were less than 100 ppm. Carry over of char nitrogen from the primary flame might be a possible source. These results suggest that the release of nitrogen from the coal residue is a minor contributor to HCN formation, in contrast to the staged combustion case[7], where its contribution may be major.

One source of HCN formation is the destruction of NO by hydrocarbon reactions. In order to explore other possible sources of HCN formation, some experiments involved a natural gas flame where the primary NO could be adjusted by doping with NH_3. In Fig. 3, the primary NO is only 24 ppm, but the HCN produced in the reburning zone is in excess of 40 ppm, corresponding to fractional conversions much higher than 100%, relative to the primary NO level. Thus, nitrogenous species inter-conversion reactions cannot account for all the formation of HCN. Clearly, Fenimore[12] fixation of N_2 produces HCN which can limit the destruction of nitrogenous species by reburning, and this agrees with the interpretation of package boiler results by Lanier et al.[5]. Figure 4 shows the effects of changes in NO_p and is used later to compare with the predictions of a model.

DATA ANALYSIS AND MODEL DEVELOPMENT

Slow Kinetic Regime (No Mixing Complications)

For this regime we take as our initial point the first data point after reburning fuel has been introduced, and attempt to predict the subsequent profiles of NO, HCN and NH_3. The objective is to determine which mechanisms control the conversion of nitrogenous species in long time scales.

Following Bose and Wendt[7], we use the detailed kinetic mechanism of Glarborg, Miller and Kee[8] (GMK) as a basis for determining both which reactions were likely to be most important and all the kinetic rate coefficients employed here. No adjustment of any rate constant is made and the analysis is done only in terms of known detailed kinetic mechanisms taken from the literature.

The rate of destruction of NO is given by:

$$NO + NH_i \rightarrow \text{products} \qquad i = 0,1,2 \qquad (1)$$

and

$$NO + CH_i \rightarrow \text{products} \qquad i = 0,1,2 \qquad (2)$$

NH_i and CH_i concentrations were calculated from partial equilibria:

$$NH_i + OH = NH_{i-1} + H_2O \qquad i = 1,2,3 \qquad (3)$$

$$CH_i + OH = CH_{i-1} + H_2O \qquad i = 1,2,3,4 \qquad (4)$$

The reaction N + OH = NO + H was not included since it contributed at most 2 ppm

NO under reburning conditions, as did $N + O_2 = NO + O$. Reactions involving HNO were not included.

This yields the following expression for the rate of change of NO:

$$\frac{d(NO)}{dt} = -(NO)(NH_3)\, f_1(OH,T) - (NO)(CH_4)\, f_2(OH,T) \qquad (5)$$

which depends on the local OH, CH_4, H_2, and H_2O concentrations. Functions $f_i(OH,T)$ represent the grouping of known elementary reaction rate constants and equilibrium constants.

HCN destruction rate was based on HCN + O reactions, HCN + OH reactions and the reversible reaction:

$$HCN + H = CN + H_2 \qquad (6)$$

where CN was at a pseudo stationary state derived from the reactions:

$CN + OH \rightarrow NCO + H$

$C + NO \rightarrow CN + O$

together with reaction (6). Assumption of partial equilibrium was made for:

$$HCN + OH = CN + H_2O$$

and O was assumed to be in partial equilibrium with H_2O and H_2.

HCN formation rate was based on reaction (2) in addition to the reactions:

$$CH + N_2 \rightarrow HCN + N \qquad (7)$$

$$CH_3 + N \rightarrow HCN + H + H \qquad (8)$$

This yields the following expressions for the rates of change of HCN:

HCN decay rate

$$\left.\frac{d(HCN)}{dt}\right|_{decay} = - (HCN)\,[f_3(OH,T) + f_4(OH,T)] \qquad (9)$$

HCN formation rate

$$\left.\frac{d(HCN)}{dt}\right|_{formation} = (CH_4)\,[(NO)f_2(OH,T) + (N_2)f_5(OH,T) + (NH_3)f_6(OH,T)] \qquad (10)$$

N_2 was formed by reaction (1) and destroyed by reaction (7) yielding:

$$\frac{d(N_2)}{dt} = (NO)(NH_3)f_7(OH,T) - (CH_4)(N_2)f_5(OH,T) \qquad (11)$$

The rate of change of NH_3 was determined from a nitrogen balance:

$$\frac{d(NH_3)}{dt} = - \frac{d(NO)}{dt} - \frac{d(HCN)}{dt} - 2\,\frac{d(N_2)}{dt} \qquad (12)$$

The f_i all have the form

$$f_i = \Sigma_j \quad A_{ij}\, T^{N_{ij}} \exp(B_{ij}/T)\, (OH)^{m_{ij}}/(H2O)^{l_{ij}}$$

where values for parameters are shown on Table I, which has been included for completeness. Equations (5 and 9-12) can predict XN species profiles, ab initio, provided initial conditions and estimates for OH are available. This is an extension of the previous analysis[7] which utilized measured NH_3 profiles, an empirical correlation for OH estimation and did not account for HCN formation due to reactions (7 and 8).

Curve A on Fig. 5 shows predictions based on OH being at equilibrium. Curve B uses an empirical correlation for the OH equilibrium overshoot[7], while curves C and D calculate the OH concentration directly via:

$$OH + H + M \rightarrow H_2O + M \tag{13}$$

which was found to be the rate controlling OH recombination reaction[13]. H was in partial equilibrium with H_2O and H_2. This yields the following expression for OH decay:

$$\frac{d(OH)}{dt} = -(H_2)f_8(OH,T) \tag{14}$$

where the initial OH concentration was calculated using measured NO decay rates from the gas flame data only, subsequent kinetic concentration of OH from Eq. (14), and correlations of all these values. This yielded the following correlation for initial OH values:

$$\frac{(OH)}{(OH)_{equil}} = 12.185x\ 10^{-6}\ \exp(19109/T) \tag{15}$$

Simultaneous solution of the rates of change of OH, NO, HCN and NH_3 (Eq. 5, 9-12 and 14) gives predictions of all nitrogenous species that are independent of their measured values (except at initial conditions). Curve C on Fig. 5 excludes reactions (7 and 8), and curve D uses the expanded kinetic set described above. The NO decay is well predicted and the HCN profile does seem to require inclusion of the Fenimore thermal fixation reactions.

Comparison of the lines shown on Fig. 1 and 4 to the data, indicates that the above expressions are successful at predicting NO, HCN and NH_3 profiles in the reburning zone for a wide range of conditions, provided CH_4 is the reburning fuel. When CO or H_2 are the reburning fuels, the small changes in the measured values of the nitrogenous species and the absence of hydrocarbons do not allow an objective examination of this mechanism under these conditions. Furthermore, other reactions, possibly involving HNO might be important.

Comparison between theory and experiment for all 12 runs in which CH_4 was the reburning fuel is shown by the symbols on Fig. 6. The random scatter pattern of the prediction suggests that the model predictions are not biased towards primary fuel type or a particular nitrogenous species.

<u>Fast Kinetic Regime (Possible Mixing Complications)</u>

It is desired to predict the values of nitrogenous species at the first data point from the primary NO values. Using the above mechanism, predictions in which a lower bound of the initial OH was estimated by extrapolation, and in which the CH_4 concentration was taken either as the initial diluted value (assumes instantaneous perfect mixing) or the value at the first data point (assumes instantaneous oxidation of CH_4) yielded NO decay rates which were always <u>far too rapid</u> at the high NO_p values. Better predictions were obtained by assuming that CH_4 rose from 0 to the measured value below the injection point, which can only be true if mixing delays the contacting of NO_p with the reburning fuel. This approach yielded predictions of NO (at the first port of the reburning zone) that were scattered around measured values with an $r^2 = 0.55$. Although the kinetic model should not be used as a predictive tool as such in this region, it demonstrates the limitations imposed by mixing on NO reduction by hydrocarbon reactions.

CONCLUSIONS

During natural gas reburning in a practical coal combustor, NO destruction occurs in two regimes, one where mixing effects may be important and limit NO destruction, followed by one downstream where a simplified kinetic scheme, based on fundamental considerations, applies for NO, HCN and NH_3 concentrations. At low primary NO values thermal fixation of N_2 by hydrocarbons limits reburning effectiveness. Hydrocarbons, however, are critical in destroying NO throughout the reburning zone which is consistent with the results of others[2,4,5] who used different experimental configurations and different primary fuels. This is in contrast to the controlling mechanisms in other coal combustion regimes, such as the fuel rich stage in air staging, where NO decay due to NH_i reactions dominates and NO reduction can be first order with respect to NO and NH_3[7,14].

The proposed mechanism can be useful in predicting and optimizing reburning effectiveness, especially if mixing both at the reburning fuel injector and at the tertiary burn out air addition point can be simulated.

FUTURE WORK

In previous work, a screening study was performed to determine the effect of various parameters on the effectiveness of the reburning process as a technique for NO_x abatement. A statistically correct experimental design was utilized for this purpose. Empirical models were derived which could predict the overall effectiveness of reburning. In this report, a kinetic model was presented which could predict the formation and destruction of all nitrogenous species in the reburn zone. The next step in this project is to extend the kinetic model in order to predict the overall effectiveness of reburning and to compare to predictions based on the derived empirical models. Furthermore, additional experiments are needed to examine reburning using nitrogen containing reburn fuels. Two sets of experiments are proposed:

1. reburning with natural gas doped with varying amounts of NH_3 and
2. reburning with coal (Bituminous or Lignite).

All the experiments conducted so far have been for a premixed primary flame configuration. In order to examine reburning under conditions that are more closely related to conditions in a practical combustor, additional reburning experiments will be conducted in the post flame of coal turbulent diffusion flames. A long axial diffusion primary flame without secondary air swirl (type A) will be investigated and the results will be interpreted in the light of findings from previous work.

REFERENCES

1. Wendt, J. O. L., Sternling, C. V. and Matovich, M. A.: Fourteenth Symposium (International) on Combustion, p. 897, The Combustion Institute, 1973.

2. Miyamae, S., Ikebe, H., Makino, K., Suzuki, K. and Mogi, J.: Proceedings of the 1985 Joint Symposium on Stationary Combustion NO_x Control, p. 24-1, EPRI, 1986.

3. Okigami, N., Sekiguchi, Y., Miura, Y., Sasaki, K. and Tamuru, R.: Proceedings of the 1985 Joint Symposium on Stationary Combustion NO_x Control, p. 25-1, EPRI, 1986.

4. Chen, S. L., McCarthy, J. M., Clark, W. D., Heap, M. P., Seeker, W. R. and Pershing, D. W.: Twenty-First Symposium (International) on Combustion, p. 1159, The Combustion Institute, 1986.

5. Lanier, W. S., Mulholland, J. A. and Beard, J. T.: Twenty-First Symposium (International) on Combustion, p. 1171, The Combustion Institute, 1986.

6. Knill, K. J. and Morgan, M. E.: The Effect of Process Variables on NO_x and Nitrogen Species Reduction in Coal Fuel Staging. Paper presented at the 1989 Joint Symposium on Stationary Combustion NO_x Control, San Francisco, CA, March, 1989.

7. Bose, A. C. and Wendt, J. O. L.: Twenty-Second Symposium (International) on Combustion, p. 1127, The Combustion Institute, 1988.

8. Glarborg, P., Miller, J. A. and Kee, R. J.: Comb. Flame, 65, 177, (1986).

9. Fenimore, C. P.: Seventeenth Symposium (International) on Combustion, p. 661, The Combustion Institute, 1979.

10. Haynes, B. S., Comb. Flame, 28, 31 (1977).

11. Haynes, B. S., Comb. Flame, 28, 113 (1977).

12. Fenimore, C. P.: Thirteenth Symposium (International) on Combustion, p. 373, The Combustion Institute, 1973.

13. Bose, A. C.: Pulverized Coal Combustion: Fuel Nitrogen Mechanisms in the Rich Post-Flame. Ph.D. Dissertation, University of Arizona, 1989.

14. Bose, A. C., Dannecker, K. M., and Wendt, J. O. L.: J. Energy Fuel, 2, 301 (1988).

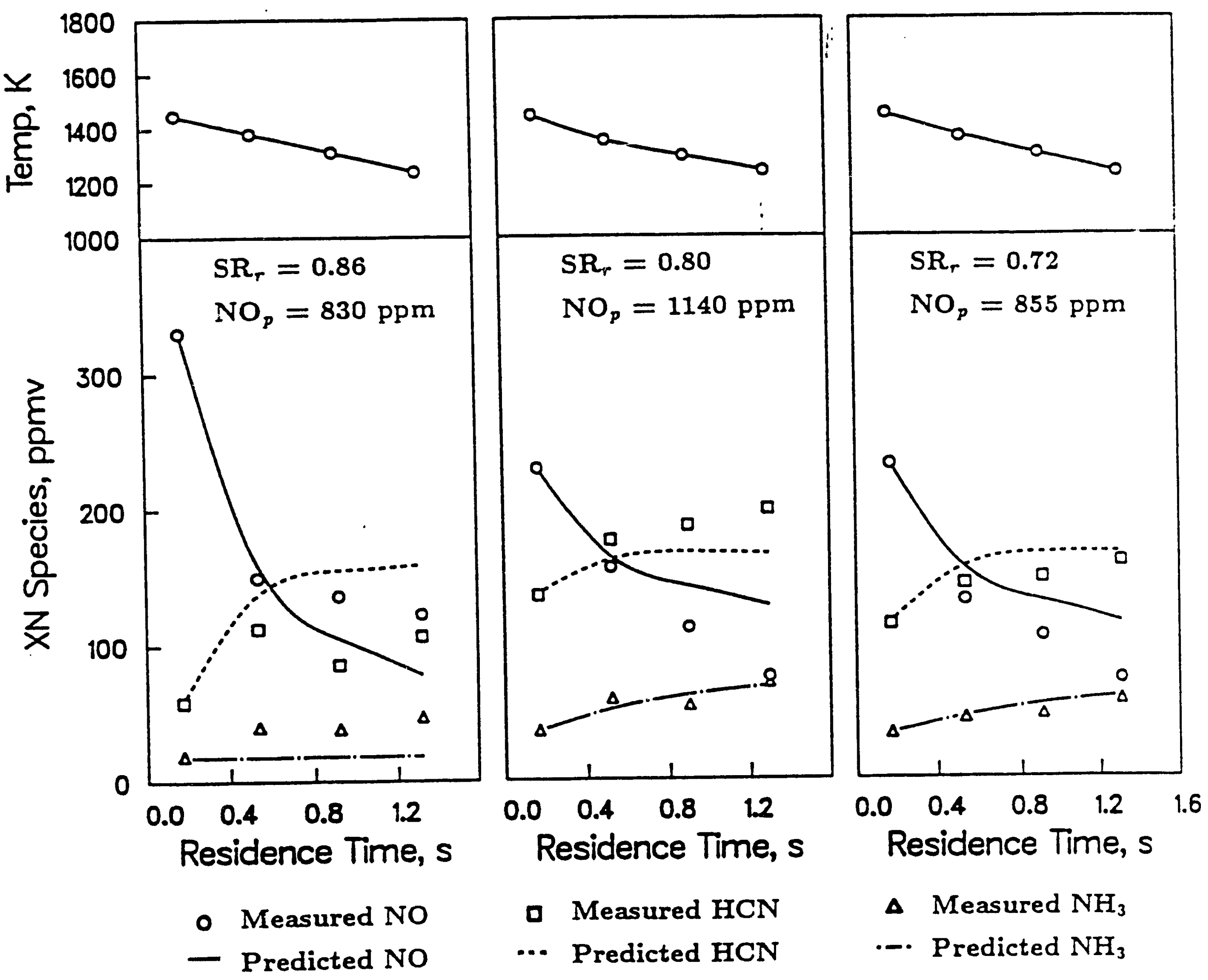

FIG. 1. Fixed Nitrogen Species Profiles in the Reburn Zone—Bituminous Coal/Natural Gas.

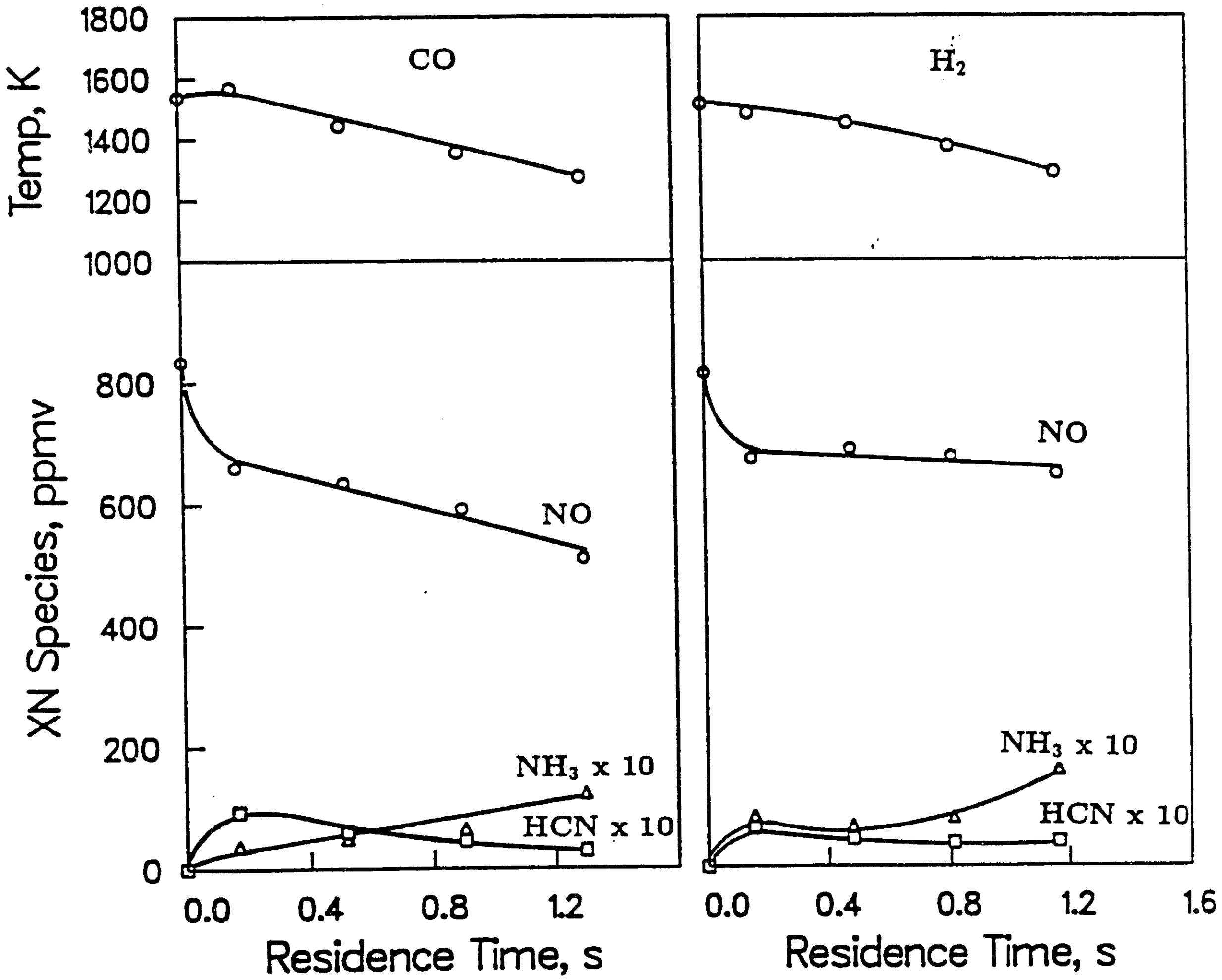

FIG. 2. Fixed Nitrogen Species Profiles in the Reburn Zone–Bituminous Coal/Non-Hydrocarbon Gas for SR_r=0.90 and $NO_p \approx 825$ ppm.

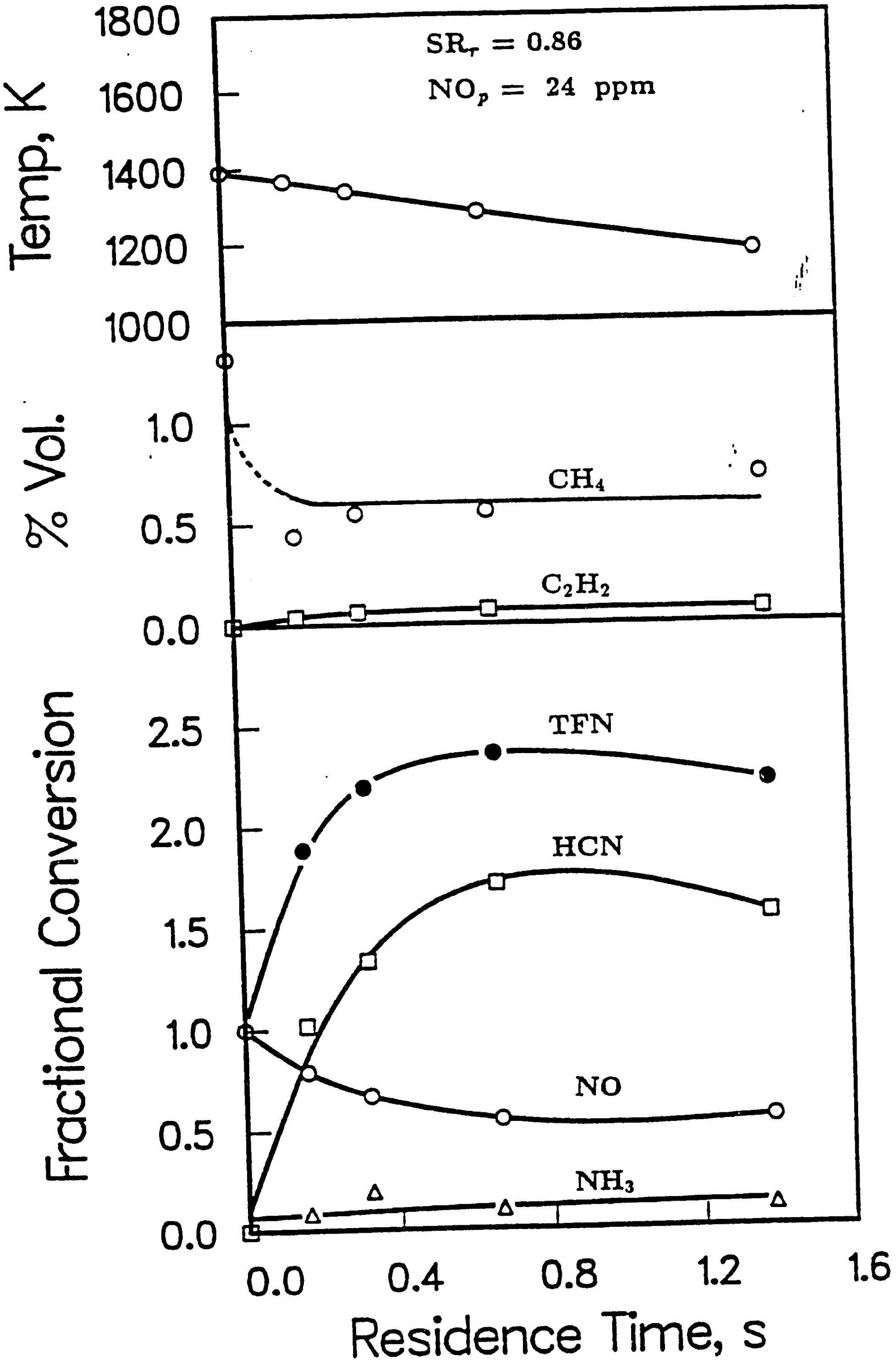

FIG. 3. Fixed Nitrogen Species Profiles in the Reburn Zone–Natural Gas/Natural Gas.

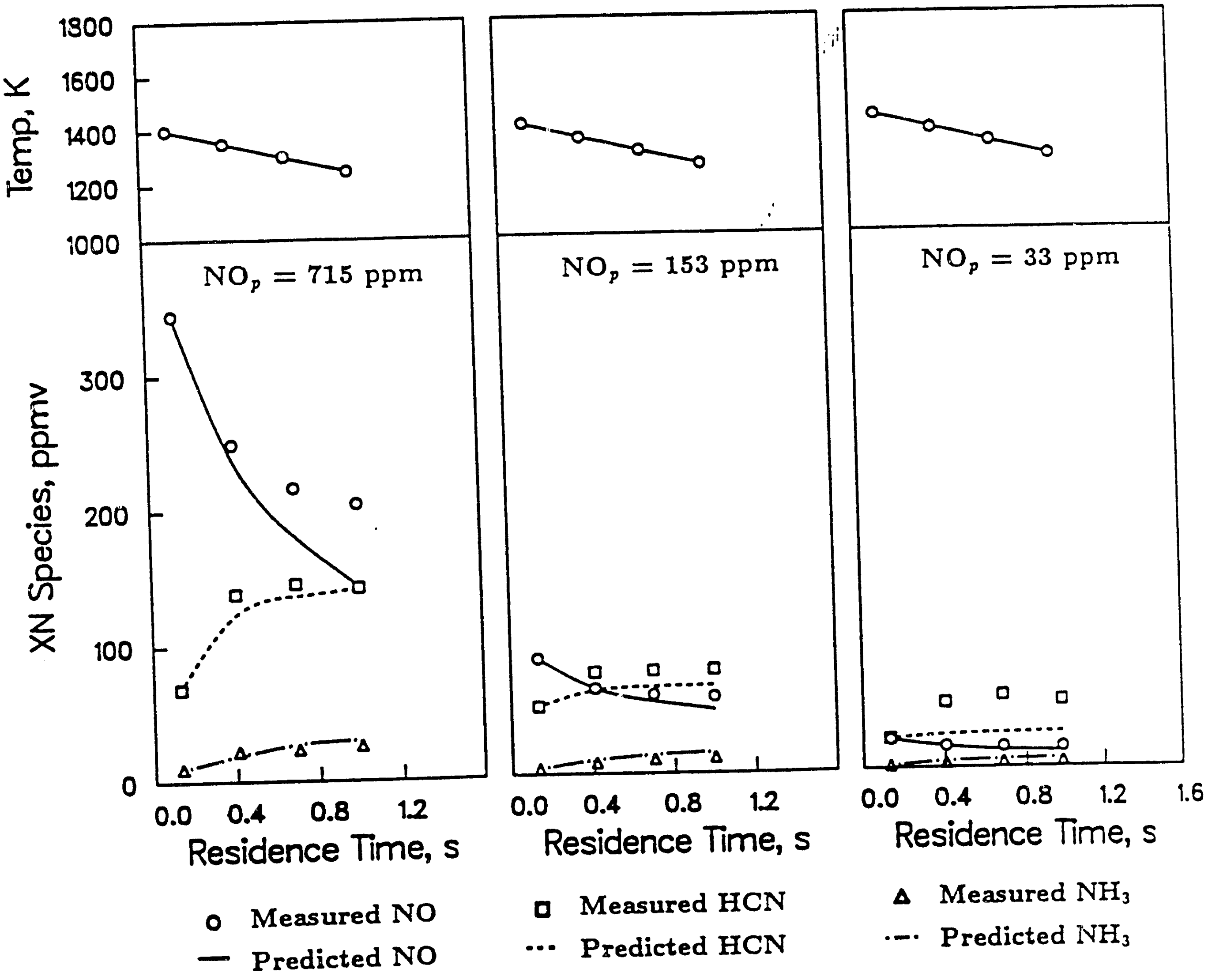

FIG. 4. Fixed Nitrogen Species Profiles in the Reburn Zone—Natural Gas + NH_3/Natural Gas for SR_r=0.87.

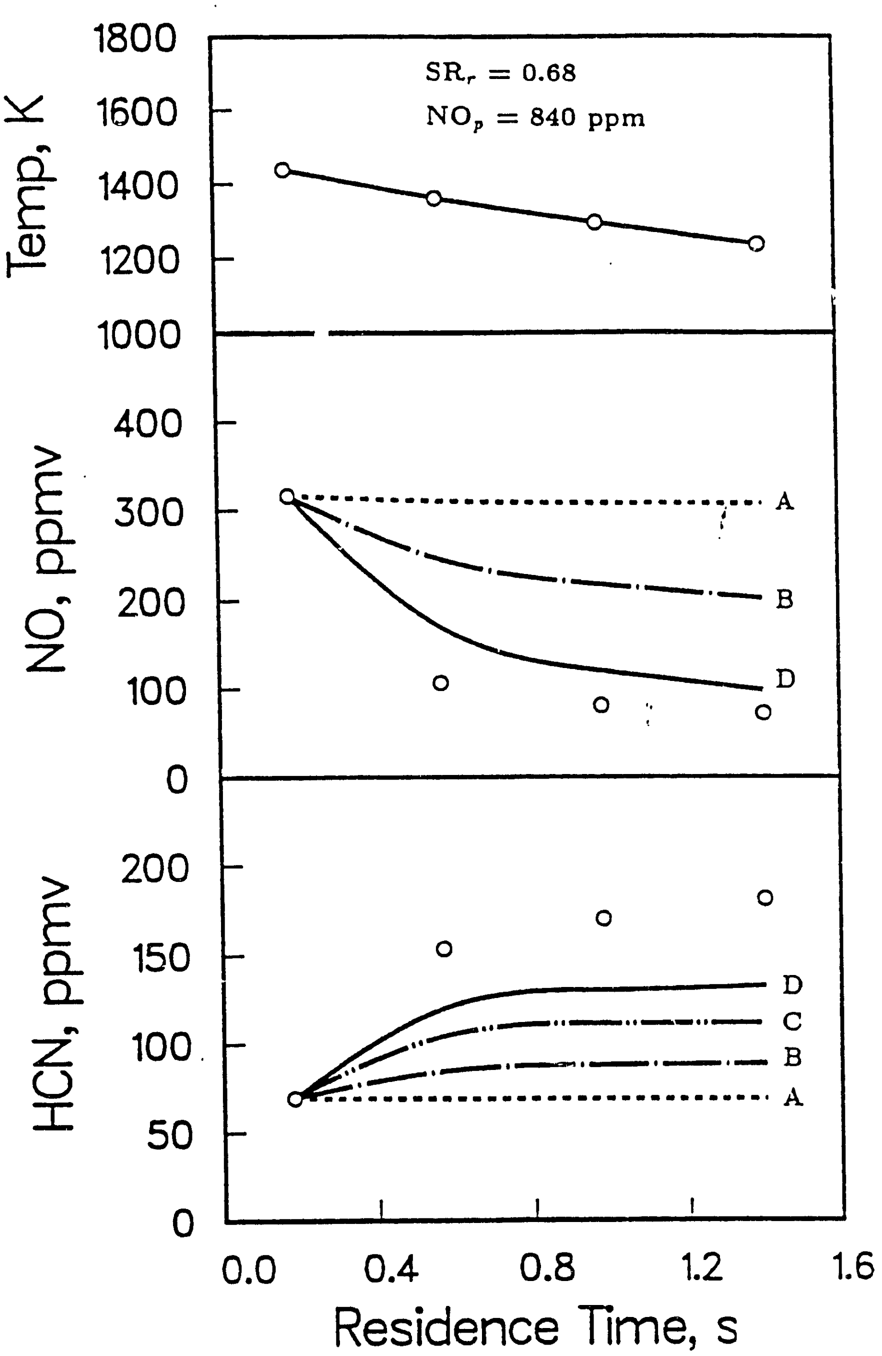

FIG. 5. Fixed Nitrogen Species Profiles in the Reburn Zone–Bituminous Coal/Natural Gas.

Symbols – Experimental Data.

Curve A – Predictions using equilibrium OH model.

Curve B – Predictions using empirical non-equilibrium OH model[7].

Curve C – Predictions using kinetic OH model.

Curve D – Predictions using kinetic OH model, expanded mechanism, see text.

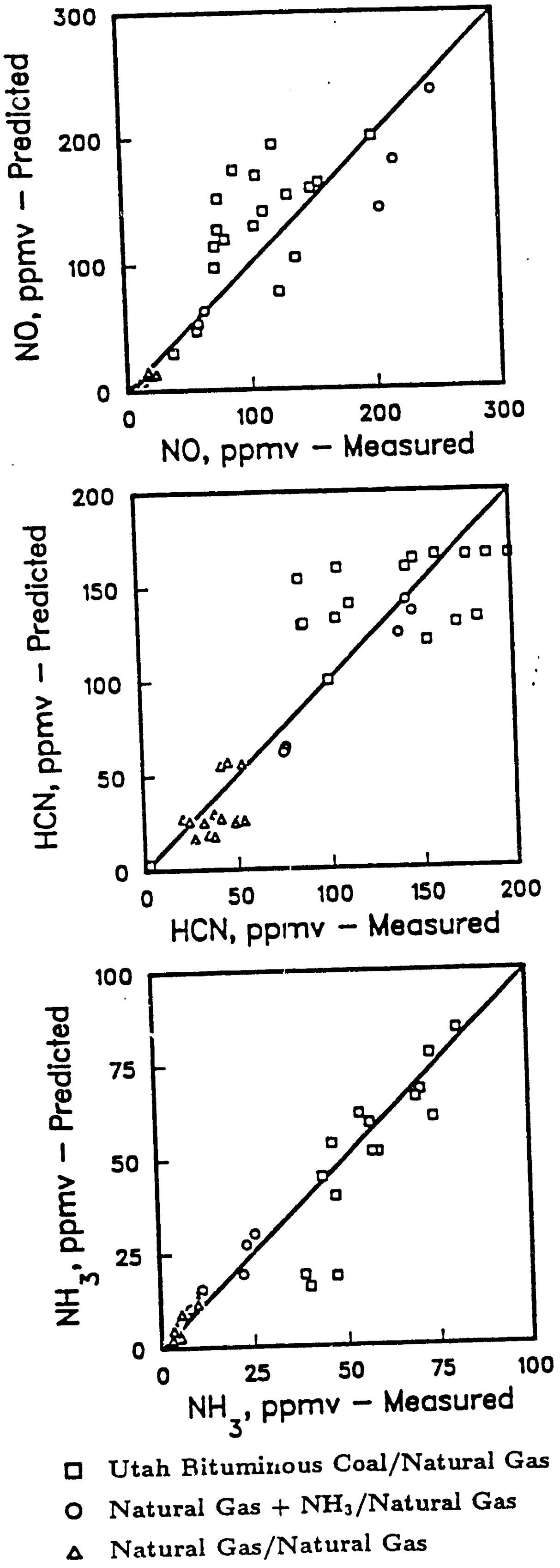

FIG. 6. Model Predictions.

TABLE I

Expressions for Functions f_i in the Form of

$$f_i = \Sigma_j \quad A_{ij} \, T^{N_{ij}} \exp(B_{ij}/T) \, (OH)^{m_{ij}}/(H2O)^{l_{ij}}$$

	j	A	N	B	m	l	units of f_i (SI)
i=1	1	3.93E+17	-1.603	5277	1	1	(cc/mol)_s^{-1}
	2	7.57E+15	-0.917	19650	2	2	
	3	3.20E+12	-0.134	39105	3	3	
i=2	1	5.83E+14	-0.484	12436	2	2	(cc/mol)_s^{-1}
	2	7.73E+16	-0.678	20730	3	3	
	3	1.20E+14	-0.292	40708	4	4	
i=3	1	9.20E+12	0	-7549	1	0	s^{-1}
	2	4.80E+11	0	-5536	1	0	
i=4	1	1.05E+03	2.701	6283	2	1	s^{-1}
	2	1.32E+16	-0.695	-1327	2	1	
i=5	1	1.34E+14	-0.678	13886	3	3	(cc/mol)_s^{-1}
i=6	1	1.25E+15	-0.603	46200	4	4	(cc/mol)_s^{-1}
i=7	1	1.18E+17	-1.603	5277	1	1	(cc/mol)_s^{-1}
	2	3.20E+12	-0.134	39105	3	3	
i=8	1	8.03E+22	-2.511	7781	2	1	(cc/mol)^2_s^{-1}

END

DATE
FILMED
2/10/92

I